Processing and Application of Ceramics 13 [4] (2019) 427–434
https://doi.org/10.2298/PAC1904427P

Processing and properties of pure antiferromagnetic h-$YMnO_3$

Milica Počuča-Nešić[1,*], Zorica Marinković Stanojević[1], Patricia Cotič Smole[2], Aleksandra Dapčević[3], Nikola Tasić[1], Goran Branković[1], Zorica Branković[1]

[1]*Institute for Multidisciplinary Research, University of Belgrade, Kneza Višeslava 1a, 11030 Belgrade, Serbia*
[2]*Institute of Mathematics, Physics and Mechanics, Jadranska 19, 1000 Ljubljana, Slovenia*
[3]*Faculty of Technology and Metallurgy, University of Belgrade, Karnegijeva 4, 11000 Belgrade, Serbia*

Received 21 June 2019; Received in revised form 1 November 2019; Accepted 6 December 2019

Abstract

Yttrium manganite ($YMnO_3$) is widely investigated multiferroic material with potential use in many technological applications. In this paper, we report on the preparation and characterization of multiferroic hexagonal YMnO3 ceramics obtained by chemical synthesis route. Precursor powders were prepared by the polymerizable complex method from citrate precursors. After calcination at 900 °C the powders contained mixture of Y-Mn-O phases which were further sintered at different temperatures. XRD analysis revealed that sintering at 1400 °C resulted in the formation of pure hexagonal $YMnO_3$. Density of the obtained ceramics was 96 %TD. The ceramic samples proved to have multiferroic properties – they are antiferromagnetic below 42 K with linear dependence of magnetization as a function of applied magnetic field. The ferroelectric measurements performed at room temperature showed remanent polarization of 0.21 μC/cm² and the coercive field of 6.0 kV/cm for the $YMnO_3$ sample sintered at 1400 °C. The magnetization curves measured at 2 and 5 K for the powder samples calcined at 900 °C and ceramic samples sintered at 1300 °C exhibited a hysteresis loop due to a small concentration of Mn_3O_4 in the samples.

Keywords: *sol-gel processes, magnetic properties, multiferroics, yttrium manganite*

I. Introduction

Multiferroics are functional materials in which two or more primary ferroic properties (ferroelectricity, ferromagnetism or ferroelasticity) simultaneously exist in the same phase [1,2]. One of the most investigated groups of this kind of materials are rare earth manganites, $REMnO_3$, (RE is rare earth element), which simultaneously exhibit ferroelectricity and magnetic properties. These materials crystallize in either hexagonal or orthorhombic crystal system in dependence on the RE ionic radius – smaller cations cause the transition from orthorhombic to hexagonal lattice [3]. Among these materials, yttrium manganite ($YMnO_3$, YMO) stands out, since the size of the Y^{3+} allows the crystallization in both crystal systems. The hexagonal structure (h-YMO, space group $P6_3cm$) is stable under ambient conditions while orthorhombic one (o-YMO, space group *Pbnm*) is metastable, but both are multiferroic. In the case of h-YMO, the Néel temperature (T_N) for the antiferromagnetic (AFM) transition is around 80 K, while the Curie temperature (T_C) for the ferroelectric transition is 914 K [4,5]. These parameters for o-YMO are 42 K (T_N) and 31 K (T_C) [5,6]. Because of its multiferroic properties YMO has become very interesting from the scientific and technological point of view with possible applications, especially in ferroelectric memory devices, magnetic storage, transducers, non-volatile memories, etc. [2,3,7].

Various synthetic methods are used for the preparation of YMO. Metastable o-YMO can be prepared either by methods involving high temperature and pressure [8–11] or by mechanochemical synthesis [12,13]. Hexagonal YMO can be prepared by solid state reactions [4,14–17], hydrothermal processes [18–20] and chemical methods [11,21–25]. Compared to other routes, chemical methods offer many advantages. They are less expensive, with simple reaction conditions. The control of product's stoichiometry can be achieved only by changing the composition of the precursor solution. Many different precursors can be used: nitrates,

* Corresponding author: tel: +381 11 2085841,
e-mail: *milicaka@imsi.bg.ac.rs*

acetates, carbonates, oxides etc. and combined with different organic/ inorganic acids and various solvents [10,11,21,22].

All these methods are applicable for the synthesis of YMO powders, but there are some challenges concerning the preparation of single phase $YMnO_3$ bulk ceramic materials. Possible change of the manganese oxidation state during the synthesis can influence the phase composition and especially magnetic properties of YMO ceramics. The existence of two or more different oxidation states of Mn with different number of *d*-electrons can violate the antiferromagnetic order in the prepared material. Also, high temperature phase transition from paraelectric to ferroelectric phase in h-YMO, which occurs during the sintering process, results in large volume change and together with highly anisotropic thermal expansion coefficients generate the microcracks in the sintered samples [26]. This phenomenon, on the other hand, strongly influences the ferroelectric properties of the sintered samples.

In this work we used polymerizable complex method (PC method), which is a modification of the well-known Pechini process [27] for the synthesis of YMO powder and ceramic samples. The aim was to prepare dense ceramic materials of single phase hexagonal YMO, to investigate their structural, magnetic and ferroelectric characteristics, correlate them with process parameters and compare obtained results with available literature data.

II. Experimental procedure

Starting materials for the YMO precursor solution were $Mn(CH_3COO)_2 \cdot 4\,H_2O$ (Sigma-Aldrich, 99.99%) and $Y(NO_3)_3 \cdot xH_2O$, (Sigma-Aldrich, 99.9%). Citric acid ($C_6H_8O_7 \cdot H_2O$, Lach-Ner, 99.8%) was used as chelating agent, while ethylene glycol ($C_2H_6O_2$, Lach-Ner, 99.8%) was used for the polyesterification reaction and as a solvent.

$Mn(CH_3COO)_2 \cdot 4\,H_2O$ was dissolved in 2 M water solution of citric acid (CA). This mixture was refluxed for three hours at 60 °C. Afterwards, the obtained precipitate was dissolved by adding concentrated ammonia, until pH value of the solution was set to 7. In this solution ethylene glycol (EG) was added to achieve Mn : CA : EG molar ratio 1 : 4 : 30.

In another beaker, $Y(NO_3)_3 \cdot xH_2O$ was dissolved in EG, and solid CA was added to the solution. Molar ratio Y : CA : EG was the same as in the case of previously prepared manganese citrate solution, i.e. 1 : 4 : 30. Final precursor solution for the preparation of YMO powder was obtained by mixing manganese and yttrium citrate solutions in equimolar metal ratio.

In order to insure mild burning and slow decomposition without organic residue, and to avoid potential material losses as a consequence of extensive foaming, prepared precursor solution was slowly dried until the gel was formed. Afterwards the dried gel was calcined at two different temperatures: 800 and 900 °C for 5 h.

For the preparation of ceramic samples only the powders calcined at 900 °C were used. They were uniaxially pressed into pellets of 6 mm in diameter at 784 MPa (8 t/cm^2), and separately sintered at 1300 °C for 10 h and 1400 °C for 2 h in air atmosphere. Based on the sintering temperature the ceramic samples are denoted as YMO1300 and YMO1400.

The calcined powders and ceramic samples were analysed by X-ray diffraction method (XRD, Ultima IV Rigaku diffractometer) and the Powder Cell software [28] was used for determination of an approximate phase composition in a Rietveld-like refinement. For further characterization of the prepared samples scanning electron microscopy (SEM, TESCAN Vega TS 5130 MM), field emission scanning electron microscope (FESEM, JEOL, Model JSM-6701F) and transmission electron microscopy (TEM JEOL, Model 2010) were used. Magnetic measurements of the prepared samples and pure Mn_3O_4 sample (Sigma-Aldrich, 97%) were carried out with a SQUID MPMS-XL-5 magnetometer from Quantum Design. The zero-field-cooled (ZFC) and field-cooled (FC) magnetization vs. temperature curves were studied in the temperature range 2–300 K, while isothermal magnetization measurements were recorded between −50 kOe and 50 kOe at two temperatures, 2 or 5 and 300 K. Standard bipolar hysteresis measurements of the ceramic samples were performed on Precision Multiferroic Test System (Radiant Technologies, Inc.), consisting of Multiferroic Test Unit and the High Voltage Amplifier up to 4000 V. The hysteresis period varied up to 250 ms and the applied field was 15 kV. Thin layer of silver paste was applied on both polished surfaces of the samples before measurements, followed by burnout of the organic paste ingredients at 150 °C, while the sample holder was made of platinum, providing good electrical contacts.

III. Results and discussion

The XRD pattern of the powder calcined at 800 °C (Fig. 1) shows that the crystallization process has started, but it is not completed yet at this temperature since the large amount of amorphous phase is still present in the sample. The main reflections belonging to orthorhombic and hexagonal phases of $YMnO_3$ can be observed, together with weak reflections of YMn_2O_5.

Increasing the calcination temperature to 900 °C resulted in better crystallization of material (Fig. 1). According to the XRD analysis, this powder contains 58 wt.% of o-$YMnO_3$ (PDF #20-0732), 20 wt.% of h-$YMnO_3$ (PDF #25-1079) and 22 wt.% of YMn_2O_5 (PDF #34-0667). Due to the better crystallinity the powder calcined at 900 °C was further used for the preparation of ceramic samples.

The morphology of YMO powder calcined at 900 °C was analysed by means of electron microscopy. FE-SEM micrographs (Fig. 2) show well crystallized ma-

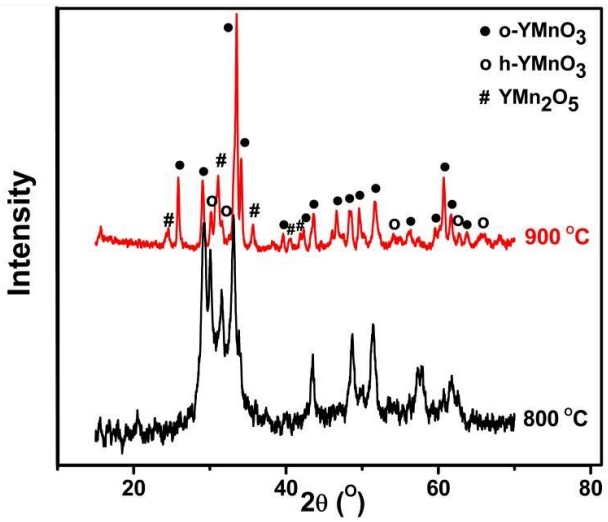

Figure 1. XRD patterns for powders calcined at 800 and 900 °C

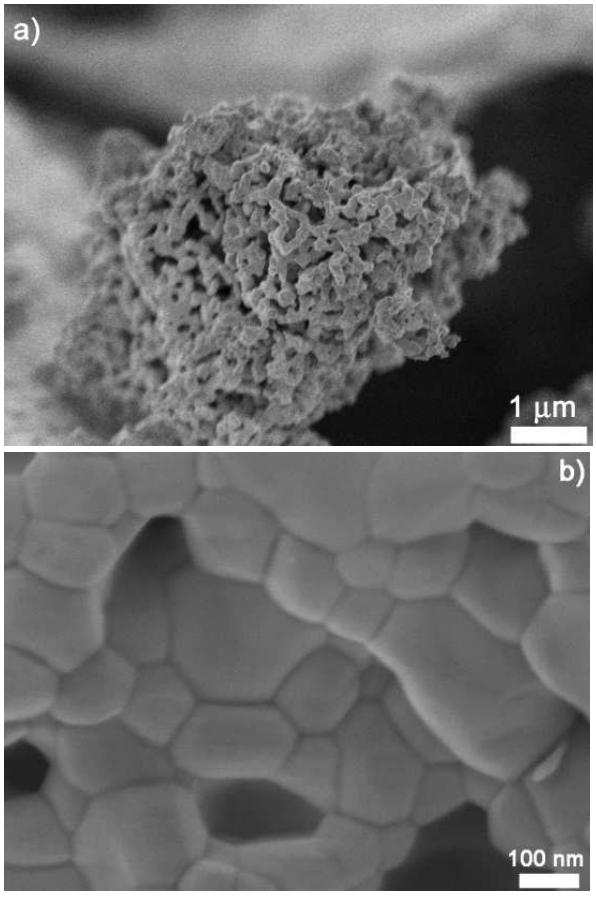

Figure 2. FE-SEM micrographs of the YMO powder calcined at 900 °C at different magnifications: a) 15000 and b) 60000

terial. It can also be seen that material is composed of polygonally shaped particles with their size ranging between 50 and 300 nm. The results of transmission electron microscopy analysis of the powder samples calcined at 900 °C confirmed the results of XRD analysis since different Y-Mn-O phases were detected. Interplanar distances of 3.7 Å and 2.9 Å marked in Fig. 3 cor-

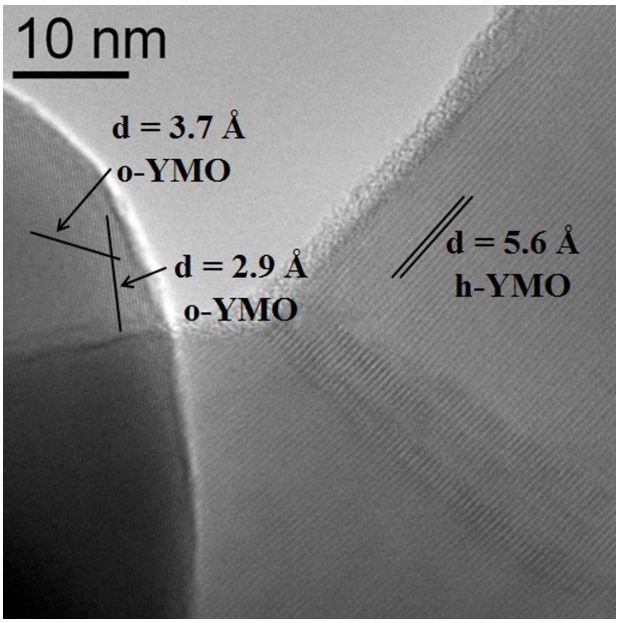

Figure 3. TEM micrograph of the prepared YMO powder calcined at 900 °C

respond to (002) and (020) crystal planes of o-$YMnO_3$, respectively, while the distance of 5.6 Å corresponds to the reflections from (002) planes of h-$YMnO_3$.

The presence of YMn_2O_5 is related to calcination temperature of 900 °C, which belongs to the temperature range of 800–1100 °C in which YMn_2O_5 is stable [29,30]. Literature data show that this compound can be formed as a secondary phase during the thermal treatment when $YMnO_3$ is synthesized in oxygen atmosphere, but not in the reduction atmosphere [21,22]. In the case of this study, the amount of atmospheric oxygen was therefore sufficient for the burning of organic material and partial oxidation of Mn^{3+} to Mn^{4+} which led to the formation of YMn_2O_5.

Figure 4a shows the magnetization curve of the YMO powder calcined at 900 °C as a function of magnetic field measured at 5 K ($M(H)$ curve). At this temperature pure YMO should show antiferromagnetic behaviour and the $M(H)$ curve should be linear. Furthermore, the mixture of three different antiferromagnetic phases such as h-YMO, o-YMO and YMn_2O_5 should also show linear dependence of the magnetization as a function of applied magnetic field. It can be seen that in our case the magnetization curve shows narrow magnetic hysteresis loop with remanent magnetization (M_R) of 0.057 emu/g and low coercive field (470 Oe), but without saturation of magnetization up to 50 kOe. The literature shows that this kind of hysteresis can exist in nanosized YMO powders [24,31] or in the presence of spin-glass state [32,33]. However, the most common reason for such behaviour is the existence of magnetic impurities present in the sample [10,22,34]. Still, the results of our XRD and FE-SEM analyses exclude these possible answers.

The thermal evolution of susceptibility for the powder calcined at 900 °C is presented in Fig. 4b. Initially, as the temperature decreases, the magnetization

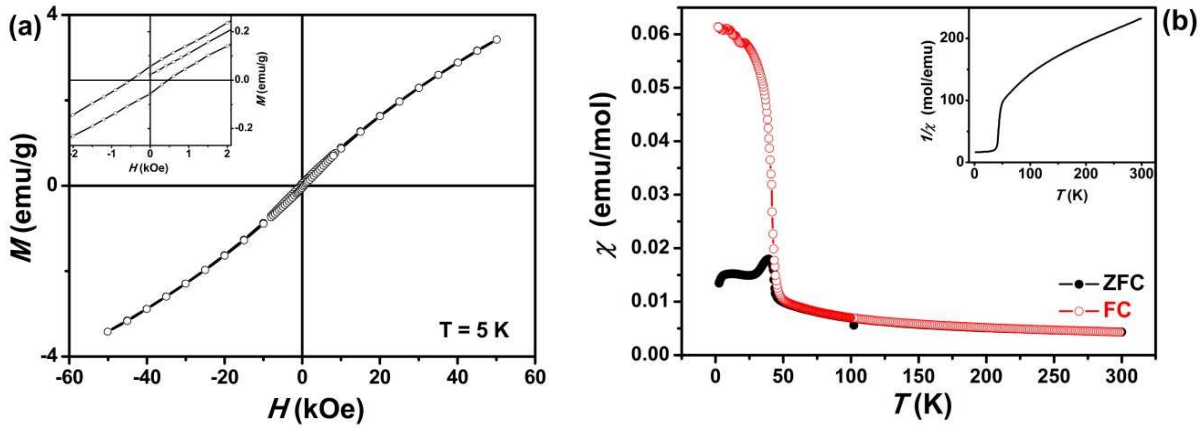

Figure 4. Magnetic properties of the YMO powder calcined at 900 °C: a) isothermal *M(H)* loop measured at 5 K (inset shows magnification of the low field region), b) susceptibility as a function of temperature, ZFC and FC cycles, measured under an applied field of 100 Oe (inset shows thermal evolution of the inverse susceptibility)

increases over the broad temperature region. At temperatures lower than 50 K, ZFC and FC curves start to separate. The measured value of the critical temperature for the calcined powder is 42 K, which is very close to the literature data for the T_N values of the two major phases in the powder: o-YMO (42 K) and YMn_2O_5 (44 K), but it also matches a transition temperature into a ferrimagnetic state of Mn_3O_4 (42 K) [4,5,22]. The values for effective magnetic moment (μ_{eff}) and the Curie-Weiss temperature (θ_{CW}) are obtained by fitting the linear part of the inverse susceptibility vs. temperature curve with the Curie-Weiss law (inset in Fig. 4b). The obtained value for θ_{CW} was −276 K, and for the μ_{eff} was 3.67 μ_B, which is below the expected value for the spin-only Mn^{3+} ions in the ground state. Lower value for μ_{eff} is the result of the existence of Mn ions with mixed oxidation states of +3 and +4. The existence of secondary phases disables superexchange reactions throughout the structure, and favours double exchange reactions between Mn^{3+} and Mn^{4+} ions [35].

The evaluation of the results of magnetic measurements points to the conclusion that calcined powder has short range antiferromagnetic order with possible presence of Mn_3O_4 as a parasitic phase.

In order to get better insight into the origin of magnetic hysteresis in the $M(H)$ curve of the powder calcined at 900 °C, we performed the magnetic measurements for the pure Mn_3O_4 commercial powder. The measured ZFC and FC susceptibility in the pure Mn_3O_4 around the transition temperature of 42 K are qualitatively similar to the ZFC-FC splitting of YMO powder calcined at 900 °C shown in Fig. 4b. We calculated the amount of Mn_3O_4 in our sample by comparing the remanent magnetizations of our YMN powder to those of the commercial Mn_3O_4 powder. The value for the remanent magnetization of the commercial powder was 30 emu/g, while it was 0.057 emu/g for our sample. Based on these results, we concluded that there was 0.2 wt.% of Mn_3O_4 in the powder calcined at 900 °C which is the value below the detection limit of XRD analysis performed for the same sample.

Results of the XRD analysis of YMO1300 ceramic sample (Fig. 5), show that its' major phase is h-YMO (94 wt.%). However, weak reflections at 36.10 and 32.39° 2θ can be attributed to the Mn_3O_4 (PDF #75-1560). The presence of 6 wt.% of Mn_3O_4 in the sample is the result of precursor powder's composition which contained YMn_2O_5. By analysing the MnO_x-$YO_{1.5}$ phase diagram it can be seen that YMn_2O_5 is stable up to 1461 K [29,36,37]. Above this temperature YMn_2O_5 decomposes to $YMnO_3$, Mn_3O_4 and O_2. The XRD pattern of YMO1400 (Fig. 5) reveals a well-crystallized single-phase material with main peaks which can be attributed to the hexagonal $YMnO_3$ with $P6_3cm$ space group.

Microstructure of the prepared ceramic samples was analysed by scanning electron microscopy. The sample YMO1300 (Fig. 6a) is composed of grains having sizes from 2 to 20 μm. The inter- and intragranular cracks [26] characteristic for this material are present in the sample beside the density of about 93 %TD. Microstructure of the surface of YMO1400 ceramic samples shows

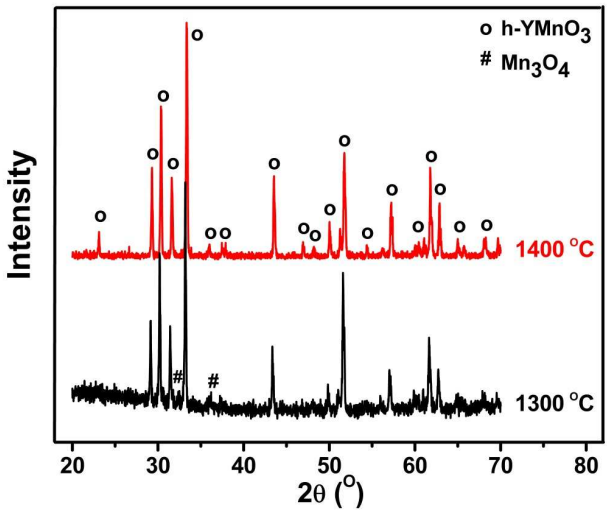

Figure 5. XRD patterns of samples sintered at 1300 and 1400 °C from YMO powder calcined at 900 °C

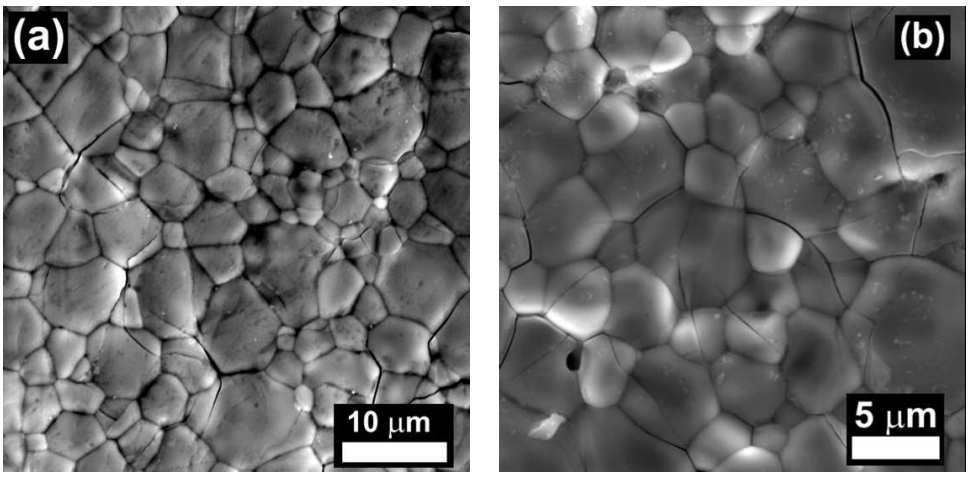

Figure 6. Microstructure of the free surfaces of samples: a) YMO1300 and b) YMO1400

similar results: well-crystallized material still with the presence of cracks (Fig. 6b). The calculated densities of these YMO ceramic samples were 96 %TD. It can be seen that grains differ in shape and size, with their size being in the range of 2 to 10 μm.

Magnetic properties of YMO1300 are strongly influenced by the presence of ferrimagnetic Mn_3O_4 (Fig. 7a). Isothermal magnetization curve taken at temperature of 300 K is in agreement with the paramagnetic behaviour of both phases above their T_N values. Contrary to the expectations, $M(H)$ curve taken at 2 K shows broad hysteresis plot with H_C = 9.4 kOe and M_R = 2.05 emu/g. With observed Neel temperature of 43 K (Fig. 7b), it is clear that magnetic properties of h-YMO are completely masked by the presence of Mn_3O_4 in the sintered sample [34].

The same method as for the determination of the amount of Mn_3O_4 present in the powder calcined at 900 °C, we used to calculate the amount of Mn_3O_4 in the YMO1300 ceramic sample. After comparing the remanent magnetization values for the commercial Mn_3O_4 and synthesized YMO1300 sample, we concluded that the YMO1300 sample contains 6.8 wt.%, which is very close to the result of the XRD analysis. This proves that magnetic measurements are sophisticated and show response for the smallest amounts of ferromagnetic or ferrimagnetic impurities in the sample, which cannot be detected by other methods.

Magnetic properties of the YMO1400 sample are presented in Fig. 8. It can be seen that at 5 K, magnetization shows linear dependence on the applied magnetic field. This is an indisputable sign of the true antiferromagnetic order in this sample. Temperature dependence of susceptibility of the YMO1400 sample is presented in Fig. 8b. ZFC and FC curves are overlapping almost throughout the whole temperature range. Reciprocal susceptibility vs. temperature curve ($\chi^{-1}(T)$) is given in the inset of Fig. 8b. The linear part of this curve above 120 K was fitted with the Curie-Weiss law, and the values for Curie-Weiss constant and effective magnetic moment were obtained. These results are: θ_{CW} = −557 K and μ_{eff} = 5.08 μ_B, which is very close to the spin-only Mn^{3+} ions in the ground state ($\mu_{Mn^{3+}}$ = 4.90 μ_B).

Magnetic measurements revealed two transition temperatures: 75 and 42 K. The first one is very close to the T_N value for h-$YMnO_3$.The second one could be the result of the existence of secondary phase whose concentration is below the detection of the XRD anal-

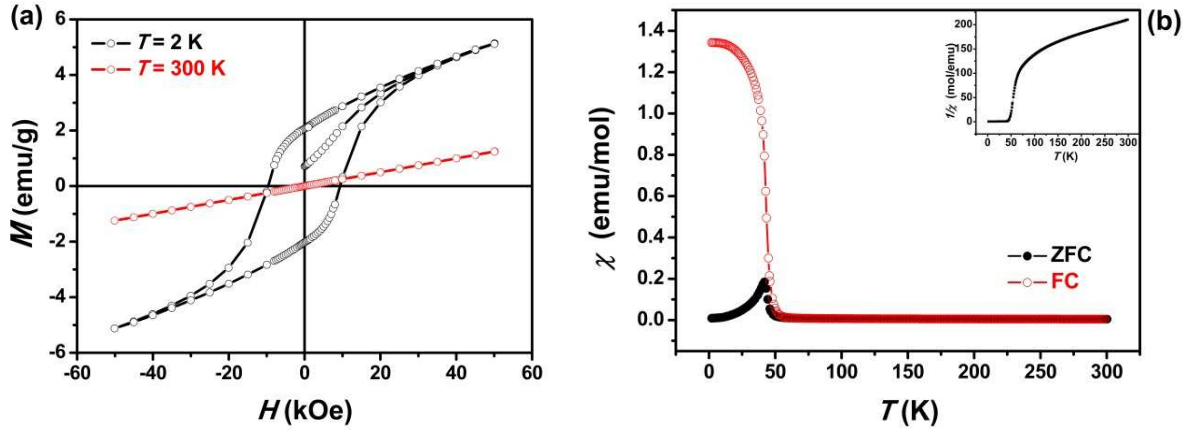

Figure 7. Magnetic properties of the YMO1300 ceramic sample: a) isothermal *M(H)* loop measured at 2 and 300 K and b) susceptibility as a function of temperature, ZFC and FC cycles, measured under an applied field of 100 Oe (inset shows thermal evolution of the inverse susceptibility)

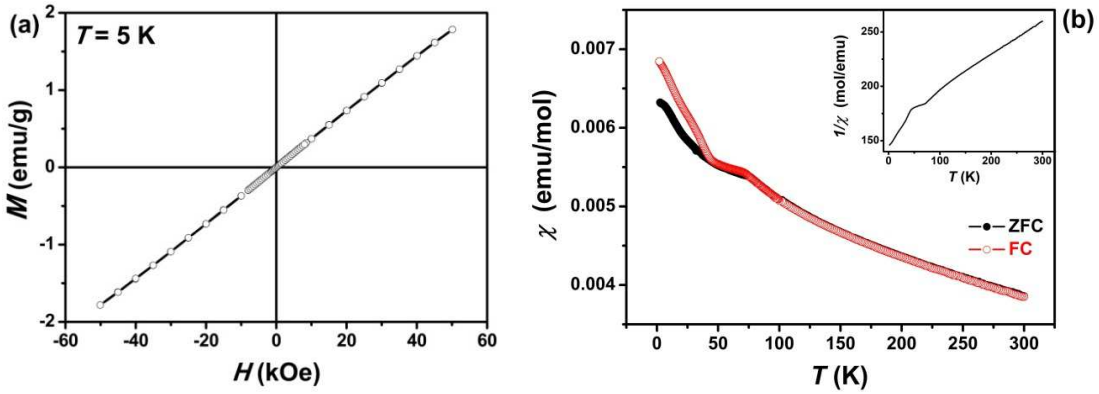

Figure 8. Magnetic properties of the YMO1400 ceramic sample: a) isothermal *M(H)* loop measured at 5 K and b) susceptibility as a function of temperature, ZFC and FC cycles, measured under an applied field of 100 Oe (inset shows thermal evolution of the inverse susceptibility)

ysis, but still can be visible by the magnetic measurements. As aforementioned, the transition temperature of 42 K matches the transition temperature values for Mn_3O_4, YMn_2O_5 and o-YMO. Since there is no hysteresis loop present in the *M*(*H*) curve we can exclude strong Mn_3O_4 as possible secondary phase. The value of the effective magnetic moment suggests the existence of manganese only in +3 oxidation state, so we concluded that there could be a small amount of orthorhombic $YMnO_3$ present in the sample.

In favour of this assumption goes the method used for the preparation of YMO ceramic samples. Polymeric precursor method used in this research was employed for the synthesis of various perovskite compounds [27,38]. The main stages of this synthetic method include the dissolution of metal salts, formation of metal–citrate complex compounds, polymerization reaction between citric acid and ethylene glycol and finally, thermal treatment. The coordination around metal ion formed in the complexation stage should remain the same all through the thermal treatment and in the final product (oxide). Based on this theoretical knowledge and ideas of some authors [10,39] it was expected that the main product of this chemical synthesis should be perovskite o-$YMnO_3$, the phase with octahedral coordination around Mn^{3+}-ion. However, Mn^{3+}-ion has unique ability to adopt five-fold coordination which results in the formation of the stable trigonal bipyramid environment and h-$YMnO_3$ [40]. Alqat *et al.* [22] obtained a mixture of o- and h-$YMnO_3$ phases using the glycine-nitrate synthesis process and the thermal treatment at 800 and 900 °C. Similar results were achieved by using different precursors like Y_2O_3 and $Mn(CO_3)_2$ [41] or chelating agents like EDTA [42], which only proves that either of two YMO phases is difficult to prepare in the single-phase form. Nevertheless, even if it has negligible amount of o-YMO, we prepared the material with true antiferromagnetic order without indications of any magnetic impurities.

Hexagonal structure of YMO consists of layers of MnO_5 trigonal bipyramids connected by in-plane O-atoms and separated by the layers of Y-atoms [43].

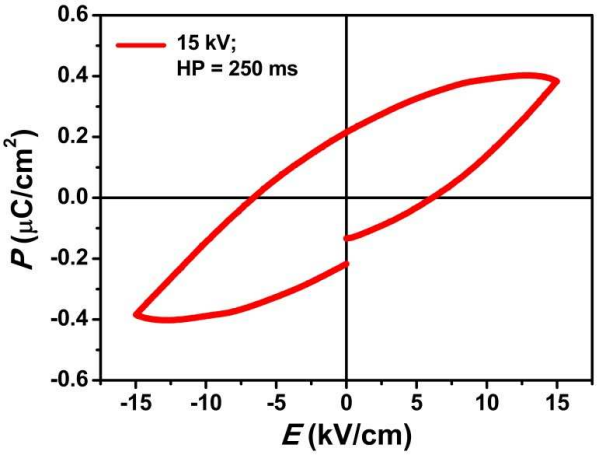

Figure 9. *P-E* hysteresis plot of YMO1400 sample measured at RT

This material is known as an improper, "geometrically driven" ferroelectric, because its ferroelectricity comes from the buckling of MnO_5 blocks and thus changes in the O–Y bonds length. The microstructure of the obtained ceramic samples, with the presence of inter- and intragranular cracks, complicates the ferroelectric characterization of the YMO ceramic samples and these materials usually show ferroelectric behaviour. The ferroelectric measurements could not be performed for the YMO1300 sample because the applied silver paste was diffusing through the pellet and formed local short circuit. The results of the ferroelectric characterization of the YMO1400 sample measured at room temperature are presented in Fig. 9.

The values for remanent polarization value and the coercive field were 0.21 μC/cm^2, and 6.0 kV/cm, respectively. These results are far from the measurements performed on the single crystal of YMO, but still are comparable to similar found in literature for polycrystalline ceramic samples [25,31,44].

IV. Conclusions

Pure multiferroic h-$YMnO_3$ ceramic material was prepared by polymeric precursor method starting from

citrate precursors. After thorough investigation, we could conclude that the method used in this investigation minimizes the possibilities of phase composition changes through the synthesis process. The powders calcined at 900 °C and sintered at 1400 °C resulted in the preparation of pure multiferroic ceramic material based on hexagonal YMO with antiferromagnetic and ferroelectric properties. Linear dependence of magnetization with applied magnetic field at 5 K confirmed the antiferromagnetic nature of the YMO ceramics. High density of these ceramic samples (96 %TD) enabled its ferroelectric characterization. Room temperature measurements revealed the remanent polarization of 0.21 μC/cm^2 and coercive field of 6.0 kV/cm for the $YMnO_3$ samples sintered at 1400 °C. Also, magnetic measurements were used for the determination of amount of Mn_3O_4 present in the calcined and sintered samples. These measurements were in accordance with XRD analyses and confirmed the assumption that weak ferromagnetism in the YMO samples often derives from the parasitic Mn_3O_4 phase.

Acknowledgement: This work was supported by Ministry of Education and Science of Republic of Serbia through project "Zero- to three-dimensional nanostructures for application in electronics and renewable energy sources: Synthesis, characterization and processing" (III45007), Bilateral cooperation between the Republic of Serbia and the Republic of Slovenia through Project "Perovskite-type transition metal oxides with multiferroic properties" (No. 651-03-1251/2012-09/21), and Slovenian Research Agency (Grant No. P2-0348).

References

1. H. Schmid, "Multi-ferroic magnetoelectrics", *Ferroelectrics*, **162** (1994) 317–338.
2. M.M. Vopson, "Fundamentals of multiferroic materials and their possible applications", *Crit. Rev. Solid State Mater. Sci.*, **40** (2015) 223–250.
3. W. Prellier, M.P. Singh, P. Murugavel, "The single-phase multiferroic oxides: from bulk to thin film", *J. Phys.: Condens. Mat.*, **17** (2005) R803–R832.
4. Z.J. Huang, Y. Cao, Y.Y. Sun, Y.Y. Xue, C.W. Chu, "Coupling between the ferroelectric and antiferromagnetic orders in $YMnO_3$", *Phys. Rev. B*, **56** (1997) 2623–2626.
5. C.C. Hsieh, T.H. Lin, H.C. Shih, C.H. Hsu, C.W. Luo, J.Y. Lin, K.H. Wu, T.M. Uen, J.Y. Juang, "Magnetic ordering anisotropy in epitaxial orthorhombic multiferroic $YMnO_3$ films", *J. Appl. Phys.*, **104** (2008) 103912.
6. M.N. Rao, N. Kaur, S.L. Chaplot, N.K. Gaur, R.K. Singh, "Lattice dynamics of orthorhombic perovskite yttrium manganite, $YMnO_3$", *J. Phys.: Condens. Mat.*, **21** (2009) 355402.
7. S.H. Kim, S.H. Lee, T.H. Kim, T. Zyung, Y.H. Jeong, M.S. Jang, "Growth, ferroelectric properties, and phonon modes of $YMnO_3$ single crystal", *Cryst. Res. Technol.*, **35** (2000) 19–27.
8. D. Okuyama, S. Ishiwata, Y. Takahashi, K. Yamauchi, S. Picozzi, K. Sugimoto, H. Sakai, M. Takata, R. Shimano,Y. Taguchi, T. Arima, Y. Tokura, "Magnetically driven ferroelectric atomic displacements in orthorhombic $YMnO_3$", *Phys. Rev. B*, **84** (2011) 054440.
9. M.N. Iliev, M.V. Abrashev, H.G. Lee, V.N. Popov, Y.Y. Sun, C. Thomsen, R.L. Meng, C.W. Chu, "Raman spectroscopy of orthorhombic perovskitelike $YMnO_3$ and $LaMnO_3$", *Phys. Rev. B*, **57** (1998) 2872–2877.
10. V.E. Wood, A.E. Austin, E.W. Collings, K.C. Brog, "Magnetic properties of heavy-rare-earth orthomanganites", *J. Phys. Chem. Solids*, **34** (1973) 859–868.
11. K. Uusi-Esko, J. Malm, N. Imamura, H. Yamauchi, M. Karppinen, "Characterization of $RMnO_3$ (R = Sc, Y, Dy-Lu): High-pressure synthesized metastable perovskites and their hexagonal precursor phases", *Mater. Chem. Phys.*, **112** (2008) 1029–1034.
12. M. Počuča-Nešić, Z. Marinković Stanojević, Z. Branković, P. Cotič, S. Bernik, M. Sousa Goes, B.A. Marinković, J.A. Varela, G. Branković, "Mechanochemical synthesis of yttrium manganite", *J. Alloys Compd.*, **552** (2013) 451–456.
13. A. Moure, T. Hungria, A. Castro, J. Galy, O. Peña, J. Tartaj, C. Moure, "Doping influence on the stability of $YMnO_3$ orthorhombic perovskite obtained by mechanosynthesis", *Mater. Chem. Phys.*, **133** (2012) 764–771.
14. D.P. Kozlenko, S.E. Kichanov, S. Leeb, J.G. Park, V.P. Glazkov, B.N. Savenko, "High-pressure effect on the crystal and magnetic structures of the frustrated antiferromagnet $YMnO_3$", *JETP Lett.*, **82** (2005) 193–197.
15. M.C. Sekhar, N.V. Prasad, "Dielectric, impedance, magnetic and magnetoelectric measurements on $YMnO_3$", *Ferroelectrics*, **345** (2006) 45–57.
16. M. Tomczyk, A.M.O.R. Senos, I.M. Reaney, P.M. Vilarinho, "Reduction of microcracking in $YMnO_3$ ceramics by Ti substitution", *Scripta Mater.*, **67** (2012) 427–430.
17. Z. Branković, G. Branković, M. Počuča-Nešić, Z. Marinković Stanojević, M. Žunić, D. Luković Golić, R. Tararam, M. Cilense, M.A. Zaghete, Z. Jagličić, M. Jagodič, J.A. Varela, "Hydrothermally assisted synthesis of $YMnO_3$", *Ceram. Inter.*, **41** (2015) 14293–14298.
18. R.D. Kumar, R. Jayavel, "Low temperature hydrothermal synthesis and magnetic studies of $YMnO_3$ nanorods", *Mater. Lett.*, **113** (2013) 210–213.
19. H.W. Zheng, Y.F. Liu, W.Y. Zhang, S.J. Liu, H.R. Zhang, K.F. Wang, "Spin-glassy behavior and exchange bias effect of hexagonal $YMnO_3$ nanoparticles fabricated by hydrothermal process", *J. Appl. Phys.*, **107** (2010) 053901.
20. E.S. Stampler, W.C. Sheets, W. Prellier, T.J. Marksa, K.R. Poeppelmeier, "Hydrothermal synthesis of $LnMnO_3$ (Ln = Ho-Lu and Y): Exploiting amphoterism in late rare-earth oxides", *J. Mater. Chem.*, **19** (2009) 4375–4381.
21. B. Fu, W. Huebner, M.F. Trubelja, V.S. Stubican, "Synthesis and properties of strontium-doped yttrium manganite", *J. Mater. Res.*, **9** (1994) 2645–2653.
22. A. Alqat, Z. Gebrel, V. Kusigerski, V. Spasojevic, M. Mihalik, M. Mihalik, J. Blanusa, "Synthesis of hexagonal $YMnO_3$ from precursorobtained by the glycine-nitrate process", *Ceram. Int.*, **39** (2013) 3183–3188.
23. C. Zhang, J. Su, X. Wang, F. Huang, J. Zhang, Y. Liu, L. Zhang, K. Min, Z. Wang, X. Lu, F. Yan, J. Zhu, "Study on magnetic and dielectric properties of $YMnO_3$ ceramics", *J. Alloy. Compd.*, **509** (2011) 7738–7741.
24. T.-C. Han, W.-L. Hsu, W.-D. Lee, "Grain size-dependent magnetic and electric properties in nanosized $YMnO_3$ multiferroic ceramics", *Nanoscale Res. Lett.*, **6** (2011) 201.

25. S.H. Liu, J.C.A. Huang, X. Qi, W.J. Lin, Y.J. Siao, C.R. Lin, J.M. Chen, M.T. Tang, Y.H. Lee, J.C. Lee, "Structural transformation and charge transfer induced ferroelectricity and magnetism in annealed $YMnO_3$", *AIP Advances*, **1** (2011) 032173.
26. M. Tomczyk, A.M. Senos, P.M. Vilarinho, I.M. Reaney, "Origin of microcracking in $YMnO_3$ ceramics", *Scripta Mater.*, **66** (2012) 288–291
27. M.P. Pechini, "Method of preparing lead and alkaline earth titanates and niobates and coating method using the same to form a capacitor", *U.S. Patent 3 330 697*, July 1967.
28. W. Kraus, G. Nolze, *Powder Cell for Windows V.2.4*, Federal Institute for Materials Research and Testing, Berlin, Germany.
29. M. Chen, B. Hallstedt, L.J. Gauckler, "Thermodynamic assessment of the Mn–Y–O system", *J. Alloy. Compd.*, **393** (2005) 114–121.
30. Y. Gao, Y.J. Wu, X.M. Chen, J.P. Cheng, Y.Q. Lin, Y. Ma, "Dense YMn_2O_5 ceramics prepared by spark plasma sintering", *J. Am. Ceram. Soc.*, **91** (2008) 3728–3730.
31. T. Ahmad, I.H. Lone, M. Ubaidullah, "Structural characterization and multiferroic properties of hexagonal nanosized $YMnO_3$ developed by a low temperature precursor route", *RSC Advances*, **5** (2015) 58065.
32. N.K. Swamy, N.P. Kumar, P.V. Reddy, M. Gupta, S.S. Samatham, D. Venkateshwarulu, V. Ganesan, V. Malik, B.K. Das, "Specific heat and magnetocaloric effect studies in multiferroic $YMnO_3$", *J. Therm. Anal. Calorim.*, **119** (2015) 1191–1198.
33. W.R. Chen, F.C. Zhang, J. Miao, B. Xu, X.L. Dong, L.X. Cao, X.G. Qiu, B.R. Zhao, P. Dai, "Re-entrant spin glass behavior in Mn-rich $YMnO_3$", *Appl. Phys. Lett.*, **87** (2005) 042508.
34. D.G. Tomuta, S. Ramakrishnan, G.J. Nieuwenhuys, J.A. Mydosh, "The magnetic susceptibility, specific heat and dielectric constant of hexagonal $YMnO_3$, $LuMnO_3$ and $ScMnO_3$", *J. Phys.: Condens. Mat.*, **13** (2001) 4543–4552.
35. A. Munoz, J.A. Alonso, M.J. Martinez-Lope, M.T. Casais, J.L. Martinez,M.T. Fernandez-Diaz, "Magnetic structure of hexagonal $RMnO_3$ (R = Y, Sc): Thermal evolution from neutron powder diffraction data", *Phys. Rev. B*, **62** (2000) 9498.
36. L.B. Vedmid', A.M. Yankin, O.M. Fedorova, V.F. Balakirev, "Evolution of phase equilibrium states in the Y–Mn–O system in the thermal dissociation of the compound YMn_2O_5", *Russ. J. Inorg. Chem.*, **59** (2014), 519–523.
37. O.M. Fedorova, V.F. Balakirev, Yu.V. Golikov, "Homogeneity regions of yttrium and ytterbium manganites in air", *Russ. J. Inorg. Chem.*, **56** (2011), 173–175.
38. L.W. Tai, P.A. Lessing, "Modified resin-intermediate processing of perovskite powders: Part I. Optimization of polymeric precursors", *J. Mater. Res.*, **7** (1992) 502–510.
39. H.W. Brinks, H. Fjellvåg, A. Kjekshus, "Synthesis of metastable perovskite-type $YMnO_3$ and $HoMnO_3$", *J. Solid State Chem.*, **129** (1997) 334–340.
40. H.L. Yakel, W.C. Koehler, E.F. Bertaut, E.F. Forrat, "On the crystal structure of the manganese (III) trioxides of the heavy lanthanides and yttrium", *Acta Cryst.*, **16** (1963) 957–962.
41. A. Munoz, J.A. Alonso, M.T. Casais, M.J. Martinez-Lope, J.L. Martinez, M.T. Fernandez-Diaz, "The magnetic structure of $YMnO_3$ perovskite revisited", *J. Phys.: Condens. Mat.*, **14** (2002) 3285–3294.
42. S.F. Wang, H. Yang, T. Xian, X.Q. Liu, "Size-controlled synthesis and photocatalytic properties of $YMnO_3$ nanoparticles", *Catal. Commun.*, **12** (2011) 625–628.
43. B.B. Van Aken, T.T.M. Palstra, A. Filippetti. N.A. Spaldin, "The origin of ferroelectricity in magnetoelectric $YMnO_3$", *Nat. Mater.*, **3** (2004) 164–170.
44. N. Kumar, A. Gaur, G.D. Varma, "Enhanced magnetization and magnetoelectric coupling in hydrogen treated hexagonal $YMnO_3$", *J. Alloys Compd.*, **509** (2011) 1060–1064.